

We are IntechOpen, the world's leading publisher of Open Access books Built by scientists, for scientists

6,900

Open access books available

186,000

International authors and editors

200M

Downloads

Our authors are among the

154

Countries delivered to

TOP 1%

most cited scientists

12.2%

Contributors from top 500 universities



WEB OF SCIENCE™

Selection of our books indexed in the Book Citation Index
in Web of Science™ Core Collection (BKCI)

Interested in publishing with us?
Contact book.department@intechopen.com

Numbers displayed above are based on latest data collected.
For more information visit www.intechopen.com



An Impact Motion Generation Support Software

Teppei Tsujita, Atsushi Konno, Yuki Nomura,
Shunsuke Komizunai, Yasar Ayaz and Masaru Uchiyama
Tohoku University
Japan

1. Introduction

When a robot applies force statically on a target object, magnitude of the force is limited by the maximum force or torque of the actuators. In order to exert a large force on the target beyond this limitation, it is effective to apply impulsive force. We describe the motions that perform tasks by applying impulsive force as “impact motion.” There are difficult problems introduced by impacts between a robot and a target.

Uchiyama proposed a control algorithm constitution method and dynamic control modes for performing a nailing task by a 3 DOF manipulator (Uchiyama, 1975). Zheng and Hemami discussed mathematical modelling of a robot that collides with the environment (Zheng & Hemami, 1985). Asada and Ogawa proposed the *virtual mass* for analyzing dynamic behaviour of a manipulator arm and its end effector that interacts with the environment (Asada & Ogawa, 1987). Around the same time, Khatib and Burdick proposed the effective mass (Khatib & Burdick, 1986). Walker investigated the effect of different configurations of kinematically redundant arms with impact force at their end effectors during contact (Walker, 1994). These works mentioned above used rigid robotic manipulators fixed on the ground.

Yoshida and Sashida investigated impact dynamics in free-floating multibody systems in space (Yoshida & Sashida, 1993). Lew discussed about contact force control of a long-reach flexible micro/macro manipulator (Lew, 1997). These studies focused on trying to minimize the impulsive force since the force causes fatal problems in a space robot or a flexible arm.

A few attempts on tasks applying impulsive force by a humanoid robot have been reported in recent years. Arisumi et al. discussed a motion generation method for dynamic lifting by a humanoid robot based on a planar model (Arisumi et al., 2007). The strategy for lifting is based on centre of percussion for maintaining stability.

The main goal of our research is to develop a scheme to generate an optimal humanoid robot’s impact motion for a given task considering multibody dynamics. To effectively generate impact motion, impact motion generation software is developed as the first step of the impact motion research.

The developed impact motion generation support software visualizes not only a designed motion but also an experimented motion. Force and torque measured in experiments are visualized on the experimented motion. The visualized ZMP (Zero-Moment Point) (Vukobratović et al., 1990), GCoM (Ground Projection of the Center of Mass), force, moment

and difference between the designed motion and the experimental result will help a motion designer improve the designed impact motion. Nailing task is taken as examples of an impact motion. A motion of a humanoid robot to drive a nail into a wooden block with a hammer is designed using the developed software. Furthermore, the software reveals a situation at the impact. The details of the software and the nailing experiment performed by the humanoid robot are presented.

2. Features of the Impact Motion Generation Support Software

In order to generate whole body motion, many motion design software are developed. Yamane and Nakamura developed an interface for creating whole body motions for human and animal characters without reference motion (Yamane & Nakamura, 2002). By dragging a link to an arbitrary position, a whole body motion can be generated intuitively. Nakaoka et al. developed a software platform for motion composition and generated robot performances of traditional folk dances based on human performances (Nakaoka et al., 2004). These software are mainly for generation natural motions which are similar to human motions. Therefore, it is significant to design postures. However, contact velocity is significant for an impact motion in addition to postures. Thus, the developed software can design a posture and joint velocities. The details of the software are described in this section.

2.1 System Configuration

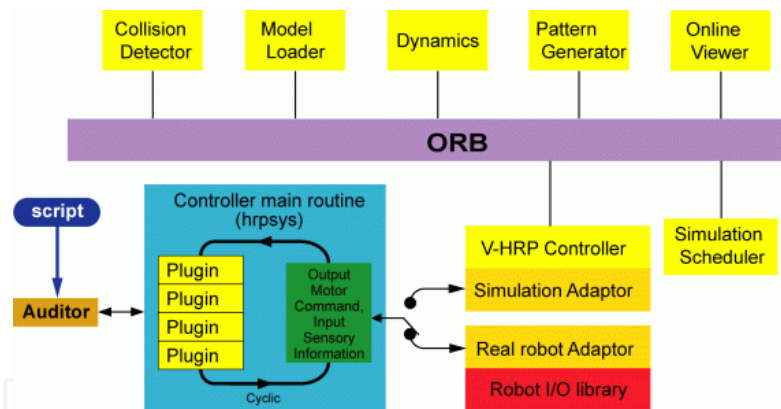


Fig. 1. Control system software of HRP-2 with OpenHRP (the figure is quoted from <http://www.generalrobotix.com/product/openhrp/products.htm>)

The impact motion generation support software is designed for a humanoid robot HRP-2 (Kaneko et al., 2004) and a humanoid robotics platform OpenHRP (Kanehiro et al., 2004). HRP-2 has 30 DOF (Degrees Of Freedom). The structure of the hands of HRP-2 used in this work is modified from that of the original HRP-2 to realize a natural swing down arm motion. The detail of the hand is described in Section 3.1. The control system software *hrpsys* and its GUI client software *Auditor* are supplied and supported by General Robotics, Inc. As shown in Figure 1, *hrpsys* is shared by HRP-2 and a dynamics simulation server. Therefore, users are able to alternate between a real robot and a simulation transparently. The impact motion generation software can be used as an add-on application of the control

system software. Figure 2 (a) shows the relationship between the generation software and the control system software.

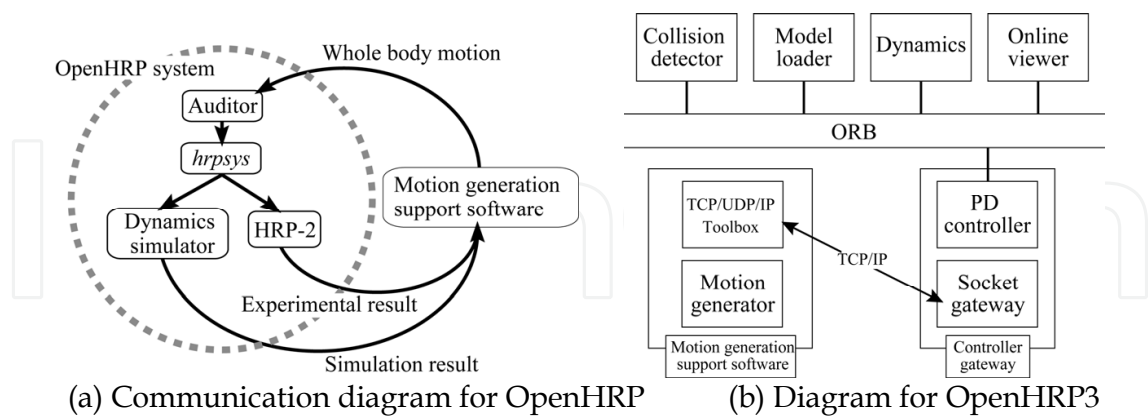


Fig. 2. A relationship between the developed software and the control system software.

The developed software consists of two main functions as follows.

- Designing the impact motion in a heuristic way
- Supporting the impact motion analysis visually

The motion design function generates a whole body motion of HRP-2. The generated motion is sent to *hrpsys* via *Auditor* for a real robot experiment or simulation. In order to analyze the motion, the results, e.g., force/torque sensor data at the wrists and ankles and measured joint angles, of the experiment or simulation are sent back to the developed software. The software is developed by using the technical computing language MATLAB R2007b (The MathWorks, Inc.). The details of these functions are described in Section 2.2 and 2.3.

2.2 Motion Design

In order to design an impact motion, the impact motion generation support software computes forward kinematics, inverse kinematics, position of the centre of mass, velocity of all links, momentum and angular momentum, GCoM (Ground Projection of the Center of Mass), ZMP (Zero-Moment Point) and a boundary of the possible region of ZMP are also computed as a measure of postural stability of the robot. The developed software is derivative of the Kajita's MATLAB toolbox for a humanoid robot (available from <http://www.ohmsha.co.jp/data/link/4-274-20058-2/>) and the MATLAB toolbox for space and mobile robots SpaceDyn (Yoshida, 1999) is referred for writing its code. The link parameters, i.e., lengths of the each link, rotation axes of the each joint, inertia matrices, masses and positions of the centre of the mass, are obtained from a VRML (Virtual Reality Modelling Language) format file of HRP-2 supplied by General Robotics, Inc. Motion is designed by deciding initial and final points of the end effector or joint angles. These descriptions are written by MATLAB script code. A designed motion is previewed with a GUI viewer. Figure 3 shows an overview of the developed software. In order to draw a HRP-2 model in a motion previewer window and obtain the parameters of the VRML format file, Virtual Reality Toolbox (The MathWorks, Inc.) is used. Virtual Reality Toolbox is a plug-in software of MATLAB that supplies functions to draw virtual reality graphics,

enabling MATLAB to control the 3D model. The designed motion is saved as a motion sequence of joints in text format. Real robot experiments or dynamics simulations are executed by loading the file on Auditor. In addition, in order to evaluate a designed motion in the full-featured dynamics simulation environment quickly, the developed software can send the joint trajectories to OpenHRP3 (Nakaoka et al., 2007) directly via TCP/IP socket communication as shown in Figure 2 (b). Simulation results, i.e., joint torques, force/moment and ZMP, are stored in MATLAB workspace directly. To handle the socket communication between the developed software and OpenHRP3, TCP/UDP/IP Toolbox (available from <http://www.mathworks.com/matlabcentral/fileexchange/345>) is used.

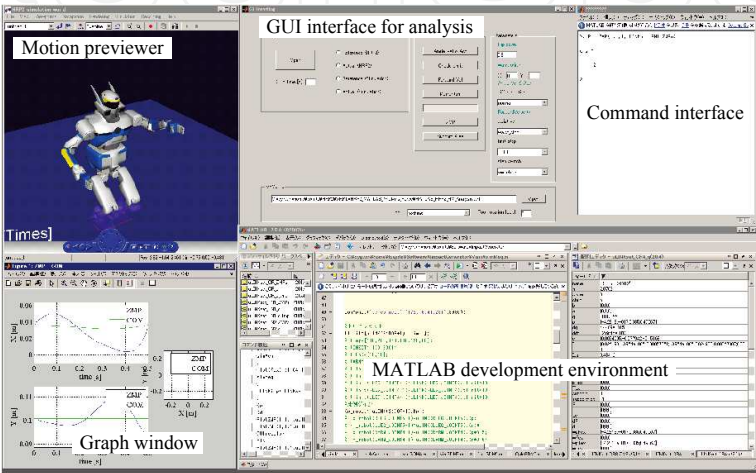


Fig. 3. An overview of the developed impact motion generation support software.

2.3 Analysis Support

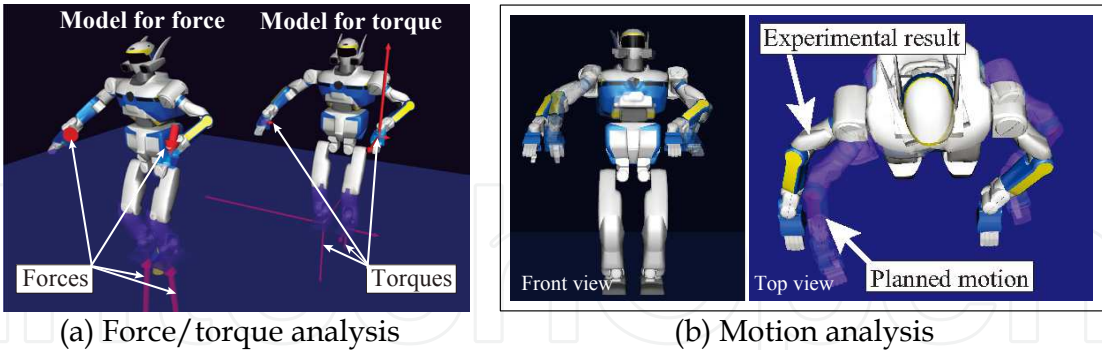


Fig. 4. Examples of force/torque and motion analysis.

It is difficult to extract significant value from enormous amount of experiment/simulation data. For instance, HRP-2 has 30 optical encoders, four force/torque sensors, a gyro sensor and an acceleration sensor (Kaneko et al., 2004). In order to clearly show what happens in an experimentation/simulation, the generation software visualizes the force/torque data, ZMP, GCoM and difference between the designed motion and the logging experimental result. The resultant sensor data are loaded from a log file recorded by a logging software of HRP-2 or the dynamics simulator using a GUI (Graphical User Interface) control panel.

Figure 4 (a) shows force and torque displayed on CG models of HRP-2. In the figure, the arrows indicate forces and torques measured by each force/torque sensor. In order to avoid confusing the force arrows with the torque ones, two HRP-2 models are displayed in the same viewer. The left model is for displaying forces, the right model is for torques. The direction and length of the arrow displayed on the left model indicates the direction and magnitude of the applied force, respectively. The pointed tops of the arrows are the position of the force sensors mounted on the wrists and the ankles. The torques are expressed by the tree orthogonal arrows. The length of the arrow indicates the magnitude of the torque around the axis. The direction of the arrow indicates rotation direction using the right-handed screw definition.

Playback speed of the reproduced motion can be variable. Slow motion is useful to understand what happens to the robot during impact phase. Due to the dynamic property of the robot, the robot may not track the designed trajectory precisely. Furthermore, end effector position is geometrically constrained at a point of collision with its environment. In order to understand the difference between the designed motion and the resultant motion intuitively, the impact motion generation support software visualizes the two motions. Figure 4 (b) shows the motion analysis viewer. In the viewer, the transparent and solid models are displayed to compare two motions. The transparent and solid models correspond to the designed motion and the resultant motion, respectively.

2.4 An example of motion generation

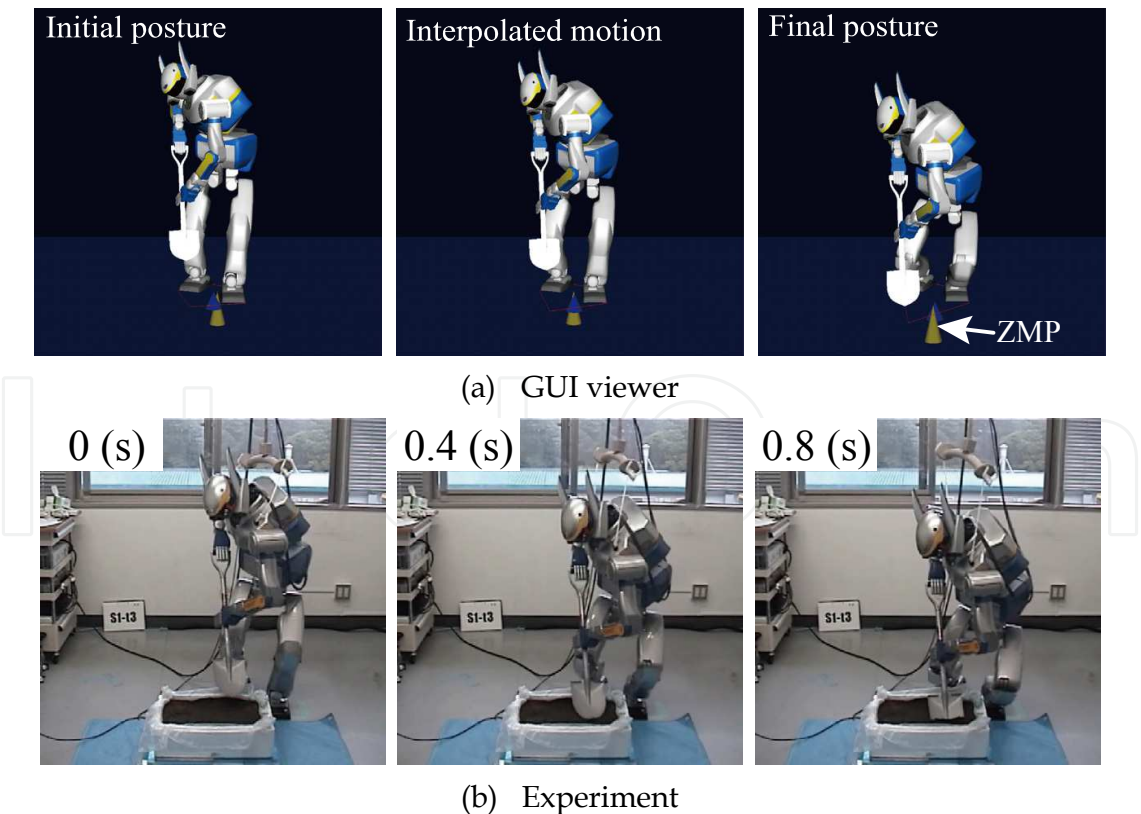


Fig. 5. HRP-2 digs a shovel blade into the dirt.

Figure 5 shows an example of motion designed by using the developed software. The motion is designed as follows.

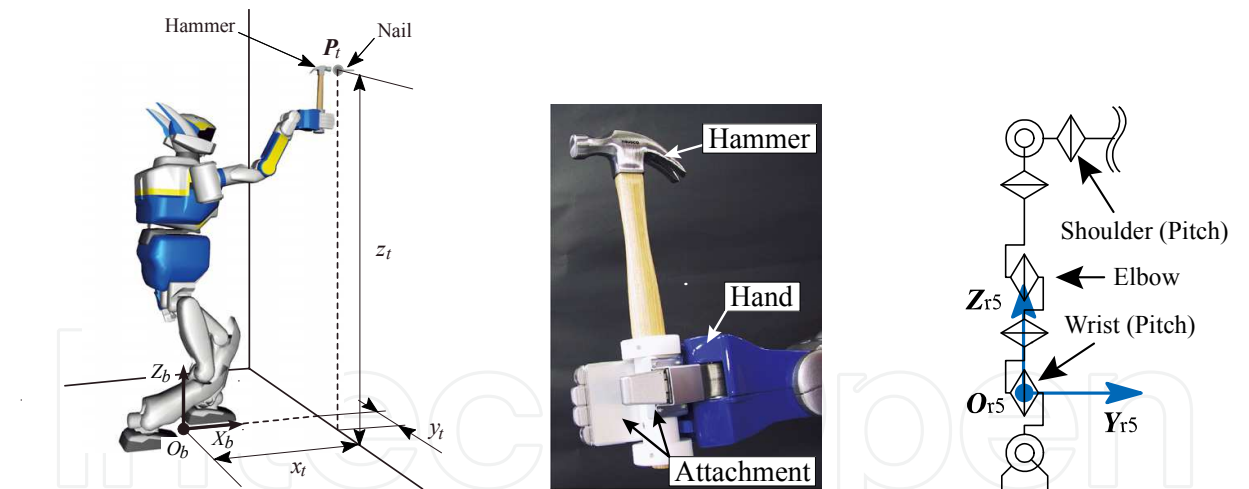
1. The initial position and orientation of the shovel and the waist are decided. The developed software computes the joint angles of the arms and the legs by solving inverse kinematics.
2. The chest joint angles are decided and a whole posture is generated by combining the arms, legs and chest joint angles.
3. The final posture is designed in the same manner.
4. The joint angles are interpolated considering the kinematics closures.

The motion can be improved without real robot experiments since ZMP position is displayed in the GUI viewer.

3. Preliminary Nailing Motion Experiment

In this section, a nailing task is taken as a case study. A nailing task is one of valuable tasks in housework, construction works, and so on. In order to evaluate the effect of reaction force and understand collision situation, the external forces and torques are gauged in the nailing task experiment.

3.1 Experimental Setup



(a) Experimented nailing task (b) HRP-2 grasps a hammer (c) Coordinate notation
Fig. 6. HRP-2 grasps a hammer by its right hand and brings down the hammer to a nail.

The robot is placed to face a wall and to drive a nail over its head as shown in Figure 6 (a). The weight of the hammer is 0.44 kg. HRP-2 grasps the hammer as shown in Figure 6 (b). Figure 7 (a) shows an experimental setup for the nailing task. A wooden block is mounted on the base at a height of about 1.3 m. The wooden block is made with 10 balsa plates whose thickness is 5 mm. A nail is driven into the wooden block. As shown in Figure 7 (b), the dimensions of the nail are 2.5 mm diameter and 45 mm long. The head of the nail is 6 mm diameter.

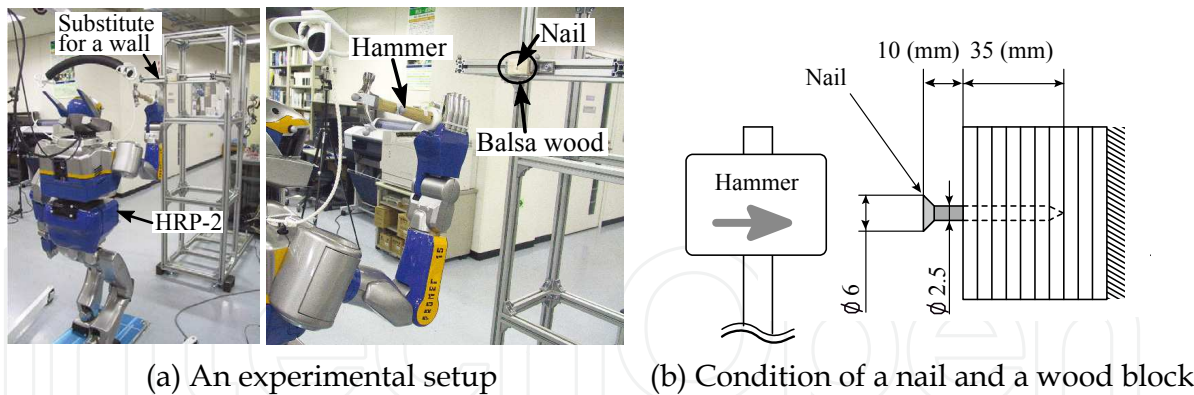


Fig. 7. A target wooden block and a nail driven by HRP-2.

3.2 Nailing Task Motion Generation

In the preliminary motion generating method, two coordinate frames are defined:

Σ_b : A reference frame fixed on the floor

$$(O_b, X_b, Y_b, Z_b),$$

Σ_{r5} : A frame fixed on the right wrist

$$(O_{r5}, X_{r5}, Y_{r5}, Z_{r5}).$$

The reference frame Σ_b is defined as illustrated in Figure 6 (a). The forward and upward direction of the robot are defined as X_b and Z_b , respectively. Y_b is defined following the right-hand rule. The wrist frame Σ_{r5} is defined as illustrated in Figure 6 (c). In order to swing the hammer, pitch joints at the shoulder, elbow, and wrist are synchronously moved.

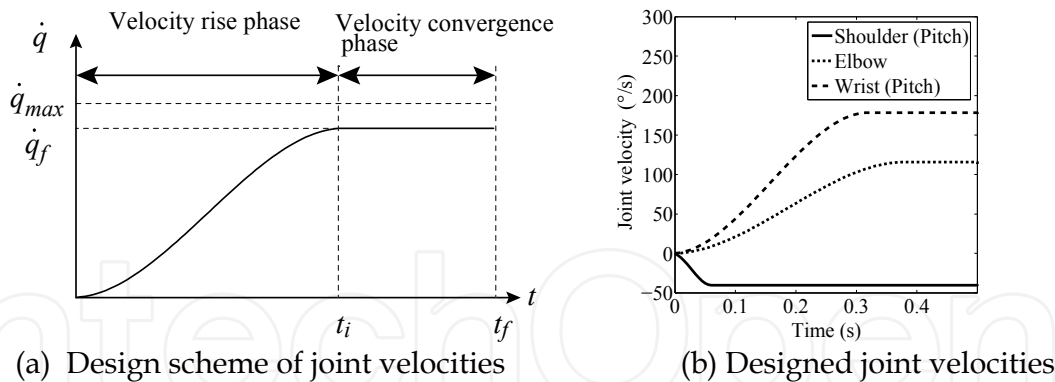


Fig. 8. Design of the shoulder, elbow and wrist joint angles.

Joint trajectories are designed in velocity domain considering the velocity limit as follows.

1. The joint velocity \dot{q}_f at the impact, the displacement of the angle from initial angle q_s to final angle q_f and the travelling time t_f are given. The joint velocity \dot{q}_s and acceleration \ddot{q}_s at the initial position are also given.
2. As shown in Figure 8 (a), the joint velocity reference is divided into velocity rise phase and velocity convergence phase.
3. The end of the rise phase t_i is derived to satisfy the displacement of the angle.

4. The joint trajectory is obtained by integrating the angle velocity reference. In step 1, \dot{q}_f is set slightly under the maximum velocity \dot{q}_{max} . \dot{q}_f is a 6×1 vector of joint angle velocities of the right arm at the impact. \dot{q}_f is derived as follows.

$$\dot{q}_f = J_{rarm}^{-1} \begin{bmatrix} v_f \\ \omega_f \end{bmatrix}, \quad (1)$$

where J_{rarm} , v_f and ω_f are respectively jacobian matrix of the right arm, velocity and rotational velocity of O_{r5} with respect to Σ_b . \dot{q}_s and \ddot{q}_s are usually set to be zero.

In step 2, since the joint velocity becomes constant before the impact, the joint acceleration \ddot{q}_f at the impact is zero and the joint velocity reaches \dot{q}_f at t_i . During the velocity rise phase, the joint velocity is interpolated with cubic interpolation.

In step 3, t_i is derived so as to fulfil the following equation:

$$\int_0^{t_i} (a_0 + a_1 t + a_2 t^2 + a_3 t^3) dt + (t_f - t_i) \dot{q}_f = q_f - q_s, \quad (2)$$

where the coefficient a_0 and a_1 are zero, since the boundary condition of cubic interpolation must satisfy $\dot{q}_s = \ddot{q}_s = 0$. The coefficient a_2 and a_3 are functions of the time t_i and the velocity \dot{q}_f as expressed by:

$$a_2 = \frac{3}{t_i^2} \dot{q}_f, \quad a_3 = -\frac{2}{t_i^3} \dot{q}_f. \quad (3)$$

Solving (2), a solution is obtained for t_i as follows:

$$t_i = \frac{2\{t_f \dot{q}_f - (q_f - q_s)\}}{t_f}. \quad (4)$$

In step 4, the joint angle q_t at the time t is obtained by integrating the angle velocity reference. If $t < t_i$, q_t is derived as follows:

$$q_t = \int_0^t \left(\frac{3}{t_i^2} \dot{q}_f t^2 - \frac{2}{t_i^3} \dot{q}_f t^3 \right) dt. \quad (5)$$

If $t \geq t_i$, q_t is derived as follows:

$$q_t = \int_0^{t_i} \left(\frac{3}{t_i^2} \dot{q}_f t^2 - \frac{2}{t_i^3} \dot{q}_f t^3 \right) dt + (t - t_i) \dot{q}_f. \quad (6)$$

3.3 Experiment

The point of driving a nail P_t is set at $x_t = 0.53$ m, $y_t = 0.23$ m and $z_t = 1.5$ m with respect to the reference frame Σ_b (Figure 6 (a)). The initial position of the point O_{r5} is set at $x_s = 0.06$ m, $y_s = 0.23$ m and $z_s = 1.4$ m with respect to the reference frame Σ_{r5} . The initial and final pose of Y_b are respectively set at -170° and -90° around the Y_b axis with respect to Σ_b . Velocity v_f and joint velocity w_f are set at $[0.3 \ 0 \ 0]^T$ m/s and $[0 \ 254 \ 0]^T$ °/s, respectively. The travelling time t_f is 0.5 s. From (1), the joint velocity \dot{q}_f is derived. Under

this condition, the time t is obtained from (4). Consequently the joint trajectories are obtained from (5) and (6). Figure 8 (b) shows the designed joint velocities of the three joints. The speed of the hammer head in X_b direction is about 1.33 m/s at the impact. To swing the hammer back to the initial position, swing up motion is designed too. The swing up motion moves the hammer head from impact point to initial position. It is designed assuming that the velocity of the hammer is zero after collision and the duration of impact is instantaneous. The nail is driven into a depth of 35 mm in advance by a human operator. Then, HRP-2 drives the remaining 10 mm into the balsa block by the above-mentioned motion as shown in Figure 9. By repeating the same motion 13 times, HRP-2 completes driving the nail.

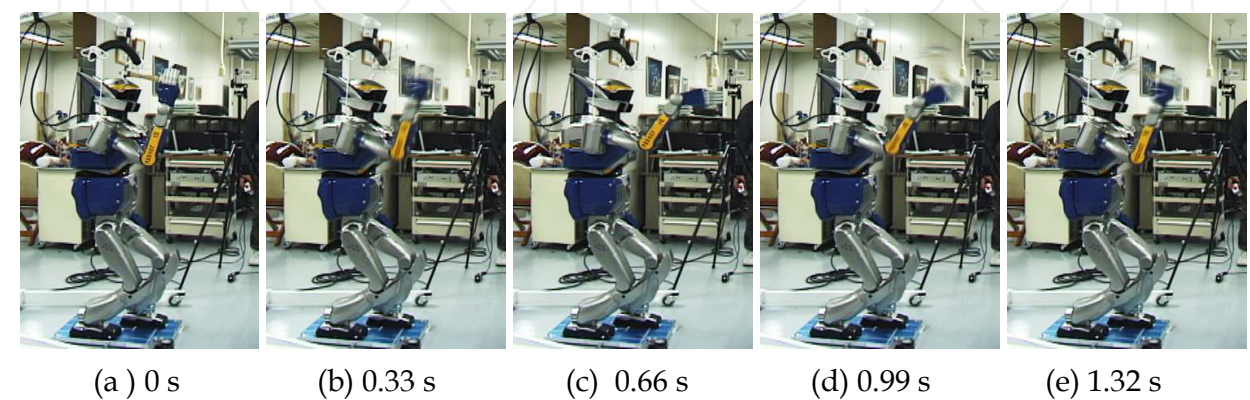


Fig. 9. HRP-2 drives a nail into a balsa wood block.

4. Analysis of Results and Problems

4.1 Motion

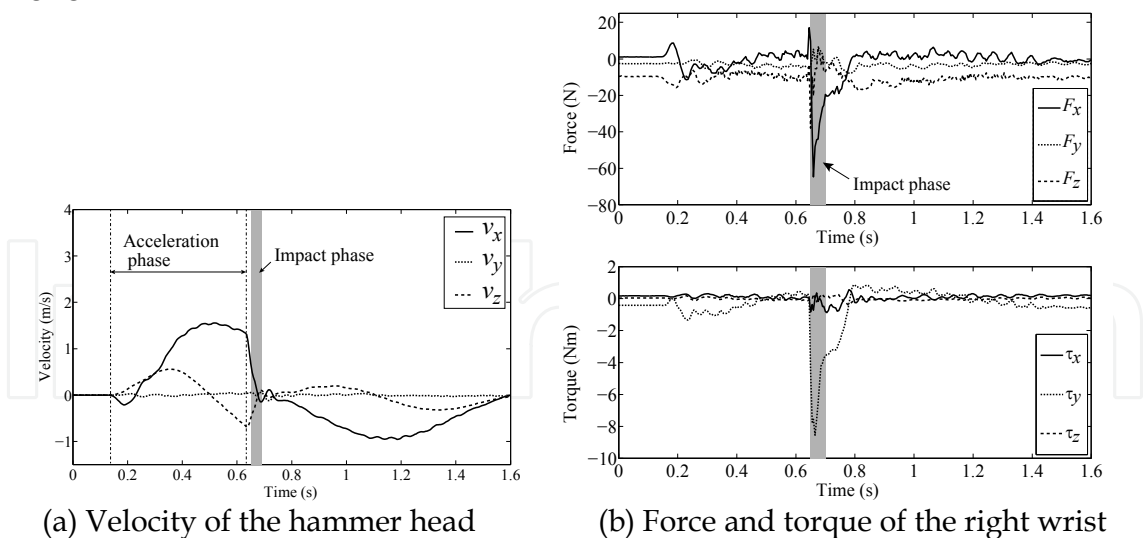


Fig. 10 Actual velocity of the hammer head computed by the joint angle velocities and force/torque measured by a sensor mounted on the right wrist.

Figure 10 (a) represents the velocity of the hammer head. The velocity is calculated by the measured joint angles and the dimensions of the hammer. At the impact (0.655 s), the hammer collides with a nail at 0.49 m/s in X_b direction. The speed is lower than expected.

The hammer trajectory is designed to collide with the nail 0.5 s after the beginning of the motion (about 0.14 s) and the speed is expected to be 1.33 m/s. This result suggests that the nail is not set in the correct place, the dimensions of the hammer are inaccurate, or the stabilizer slightly changes the trajectory of the hammer head.

4.2 Reaction Force

Figure 10 (b) shows the force and torque measured by the force/torque sensor mounted on the right wrist with respect to Σ_b . As shown in Figure 10 (b), peak of force in the negative direction of X_b is seen from 0.655 s to 0.700 s. The phase is considered as the impact phase. The duration of the impact is about 0.045 s.

Figure 11 shows the force and torque before and after contact. Before contact, large force can be seen in negative direction of Z_b . At the impact, a large force is produced in the negative direction of X_b . 5 ms after impact, peak force is measured. Experimental data show dynamic change of reaction force. Since the pulling up motion is designed assuming that the velocity of the hammer is zero after collision and the duration of impact is quite small, the acceleration is discontinuous between the swing down and up motions. Moreover, the impact happens later than expected. Therefore, it seems that the large force seen at 0.650 s is caused by inertial force. The force in X_b direction rapidly increases from 0.655 s to 0.660 s. The nail point compresses the balsa block during this phase and the balsa wood has elasticity, thus, the force increases gradually.

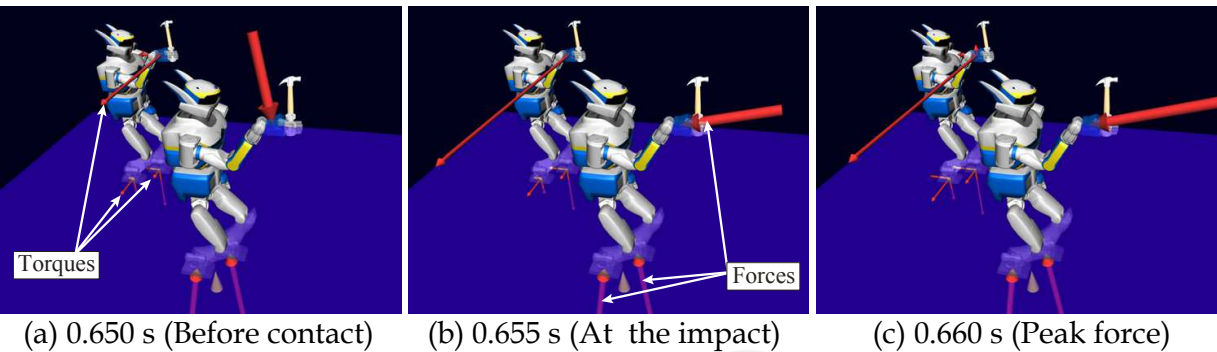


Fig. 11 Visualization of force and torque.

4.3 Stability

Figure 12 (a) shows ZMP and support polygon. The solid line, dotted line and gray box represent ZMP, support polygon and footprints, respectively. The ZMP has enough margins to the edge of the support polygon. Therefore it can be concluded that the motion is stable. Figure 12 (b) shows trajectories of ZMP. The external force affects the ZMP. In this case, since large force in the negative direction of X_b and large torque around Y_b axis are measured, the position moves to the negative direction of X_b . However, during the impact phase, significant change of the position is not observed. After about 0.07 s of the collision, peak reaction force in X_b direction is measured (0.660 s), and the ZMP in X_b direction rapidly moves from about 0.05 m to 0.01 m. This change is thought to be the effect of the reaction force. To confirm the effect of the reaction force on stability, ZMP when the hammer

does not collide with the nail are also shown in Figure 12 (b). The change of ZMP in X_b is observed after about 0.07 s of the expected moment of impact. However, the direction is opposite. This change is believed to be effect of inertial force, since the velocity of the hammer changes rapidly around the expected moment of impact. Since the deflection of ZMP at about 0.730 s depends on whether the hammer head collides with the nail or not, there is a time delay in relationships between reaction force and the stability and it is estimated to be about 0.07 s.

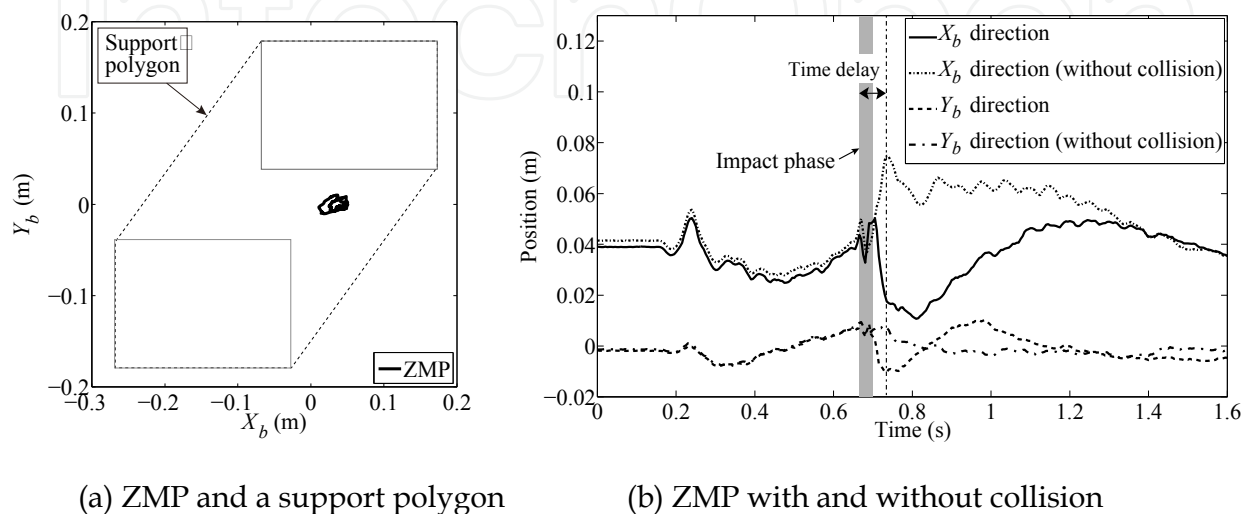


Fig. 12. Behaviour of ZMP during impact phase.

5. Conclusions

The detail of impact motion generation support software is presented in this paper. The developed software supports impact motion design with OpenHRP or OpenHRP3. A preliminary impact motion experiment is performed by a humanoid robot and the analyses of its result are presented. The analysis reveals that the designed motion is not robust against error in the position of the nail since the timing of pulling up the hammer is defined in the designed motion in advance. Therefore, a robust feedback control method for driving a nail is required.

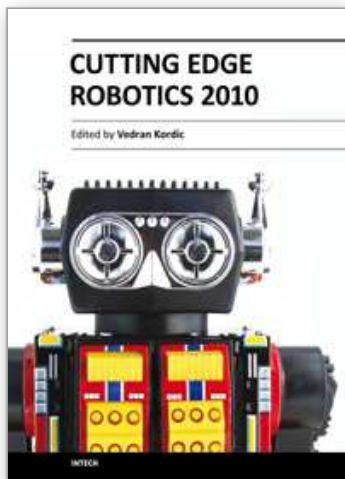
The motions which are described in this paper are designed heuristically. However, the developed software can communicate with OpenHRP3 and use MATLAB toolboxes. As a next step, an impact motion will be optimized by using these features.

6. Acknowledgement

This research was supported by NEDO Industrial Technology Research Grant Program (project ID: 05A30703a) and JSPS Grant-in-Aid for JSPS Fellows (20•6273).

7. References

- Arisumi, H.; Chardonnet, J.-R.; Kheddar, A. & Yokoi, K. (2007). Dynamic Lifting Motion of Humanoid Robots, *Proc. of Int. Conf. on Robotics and Automation*, pp. 2661-2667, ISBN 1-4244-0602-1, Roma, Italy, Apr., 2007, IEEE.
- Asada, H. & Ogawa, K. (1987). On the dynamic analysis of a manipulator and its end effector interacting with the environment, *Proc. of IEEE Int. Conf. on Robotics and Automation*, pp. 751-756, ISBN 0-8186-0787-4, NC, USA, Mar.-Apr., 1987, IEEE.
- Kanehiro, F.; Hirukawa, H. & Kajita, S. (2004). OpenHRP: Open architecture humanoid robotics platform, *Int. J. of Robotics Research*, Vol. 23, No. 2, pp. 155-165, ISSN 0278-3649.
- Kaneko, K.; Kanehiro, F.; Kajita, S.; Hirukawa, H.; Kawasaki, T.; Hirata, M.; Akachi, K. & Isozumi, T. (2004). Humanoid robot HRP-2, *Proc. of IEEE Int. Conf. on Robotics and Automation*, pp. 1083-1090, ISBN 0-7803-8232-3, CA, USA, Apr., 2004, IEEE.
- Khatib, O. & Burdick, J. (1986). Motion and force control of robot manipulators, *Proc. of IEEE Int. Conf. on Robotics and Automation*, pp. 1381-1386, ISBN 0-8186-0695-9, CA, USA, Apr., 1986, IEEE.
- Nakaoka, S.; Nakazawa, A. & Ikeuchi, K. (2004). An Efficient Method for Composing Whole Body Motions of a Humanoid Robot, *Proc. of Int. Conf. on Virtual Systems and Multimedia*, pp. 1142-1151, ISBN 978-4274906343, Gifu, Japan, Nov., 2004, Ohmsha.
- Nakaoka, S.; Hattori, S.; Kanehiro, F.; Kajita, S. & Hirukawa, H. (2007). Constraint-based Dynamics Simulator for Humanoid Robots with Shock Absorbing Mechanisms, *Proc. of IEEE/RSJ Int. Conf. on Intelligent Robots and Systems*, pp. 3641-3647, ISBN 978-1-4244-0912-9, CA, USA, Oct., 2007, IEEE.
- Uchiyama, M. (1975). A control algorithm constitution method for artificial arm and dynamic control modes, In: *Biomechanism 3*, Society of Biomechanism Japan, pp. 172-181, University of Tokyo Press, ISBN 978-4-13-060069-9 (in Japanese).
- Vukobratović, M.; Borovac, D.; Surla, D. & Stokić, D. (1990) *Biped Locomotion – Dynamics, Stability, Control and Application*, Springer-Verlag, ISBN 978-0387174563.
- Walker, I. D. (1994). Impact configurations and measures for kinematically redundant and multiple armed robot systems, *IEEE Trans. on Robotics and Automation*, Vol. 10, No. 5, Oct., 1994, pp. 670-683, ISSN 1042-296X.
- Yamane, K. & Nakamura, Y. (2002). Synergetic CG choreography through constraining and deconstraining at will, *Proc. of IEEE Int. Conf. on Robotics and Automation*, pp. 855-862, ISBN 0-7803-7272-7, DC, USA, May, 2002, IEEE.
- Yoshida, K. & Sashida, N. (1993). Modeling of impact dynamics and impulse minimization for space robots, *Proc. of IEEE/RSJ Int. Conf. on Intelligent Robots and Systems*, pp. 2064-2069, ISBN 0-7803-0823-9, Yokohama, Japan, Jul., 1993, IEEE.
- Yoshida, K. (1999). The SpaceDyn: a MATLAB toolbox for space and mobile robots, *Proc. of IEEE/RSJ Int. Conf. on Intelligent Robots and Systems*, pp. 1633-1638, ISBN 0-7803-5184-3, Kyongju, South Korea, Oct., 1999, IEEE.
- Lew, J. Y. (1997). Contact control of flexible micro/macro-manipulators, *Proc. of IEEE Int. Conf. on Robotics and Automation*, pp. 2850-2855, ISBN 0-7803-3612-7, NM, USA, Apr., 1997, IEEE.
- Zheng, Y. F. & Hemami, H. (1985). Mathematical modeling of a robot collision with its environment, *J. of Robotic Systems*, Vol. 2, No. 3, 1985, pp. 289-307, ISSN 0741-2223.



Cutting Edge Robotics 2010

Edited by Vedran Kordic

ISBN 978-953-307-062-9

Hard cover, 440 pages

Publisher InTech

Published online 01, September, 2010

Published in print edition September, 2010

Robotics research, especially mobile robotics is a young field. Its roots include many engineering and scientific disciplines from mechanical, electrical and electronics engineering to computer, cognitive and social sciences. Each of this parent fields is exciting in its own way and has its share in different books. This book is a result of inspirations and contributions from many researchers worldwide. It presents a collection of a wide range of research results in robotics scientific community. We hope you will enjoy reading the book as much as we have enjoyed bringing it together for you.

How to reference

In order to correctly reference this scholarly work, feel free to copy and paste the following:

Teppei Tsujita, Atsushi Konno, Yuki Nomura, Shunsuke Komizunai, Yasar Ayaz and Masaru Uchiyama (2010). An Impact Motion Generation Support Software, Cutting Edge Robotics 2010, Vedran Kordic (Ed.), ISBN: 978-953-307-062-9, InTech, Available from: <http://www.intechopen.com/books/cutting-edge-robotics-2010/an-impact-motion-generation-support-software>

INTECH
open science | open minds

InTech Europe

University Campus STeP Ri
Slavka Krautzeka 83/A
51000 Rijeka, Croatia
Phone: +385 (51) 770 447
Fax: +385 (51) 686 166
www.intechopen.com

InTech China

Unit 405, Office Block, Hotel Equatorial Shanghai
No.65, Yan An Road (West), Shanghai, 200040, China
中国上海市延安西路65号上海国际贵都大饭店办公楼405单元
Phone: +86-21-62489820
Fax: +86-21-62489821

© 2010 The Author(s). Licensee IntechOpen. This chapter is distributed under the terms of the [Creative Commons Attribution-NonCommercial-ShareAlike-3.0 License](https://creativecommons.org/licenses/by-nc-sa/3.0/), which permits use, distribution and reproduction for non-commercial purposes, provided the original is properly cited and derivative works building on this content are distributed under the same license.

IntechOpen

IntechOpen